RAPID COMMUNICATIONS

PHYSICAL REVIEW B VOLUME 44, NUMBER 24 15 DECEMBER 1991-II

Temperature-dependent coverage of the $\sqrt{3}\times\sqrt{3}R30°$ structure of Ag/Si(111)

G. Raynerd, M. Hardiman, and J. A. Venables*
School of Mathematical and Physical Sciences, University of Sussex, Brighton BN1 9QH, United Kingdom
(Received 13 August 1991)

The coverage Θ, of the $\sqrt{3}\times\sqrt{3}R30°$ Ag/Si(111) interface has been measured by micro-Auger electron spectroscopy. With a dose of 5 monolayer (ML), we find $\Theta\approx 1$ ML for deposition temperature $T_d \geq 700$ K and $\Theta\approx \frac{2}{3}$ ML for $T_d \leq 620$ K. Much smaller changes (≈ 0.05 ML) were observed during annealing. These effects are explained by a simple kinetic model in which ~ 2 Ag atoms are readily incorporated into the structure, but a third atom must overcome an activation energy E_r to become embedded, with a gain in energy E_e. We find $E_r = 1.90$, $E_e = 0.60$, and $E_a = 2.45$, all ± 0.05 eV, where E_a is the adatom adsorption energy. Possible structural and microstructural models and the interpretation of the energy E_r are discussed.

The Ag/Si(111) system is perhaps the most studied metal-semiconductor interface and has been subject to essentially every available surface-sensitive technique.[1-15] It is established that the $\sqrt{3}\times\sqrt{3}R30°$ structure is formed above 470 K; this interface is very stable, and little or no interdiffusion into the bulk occurs. Above the saturation coverage for the $\sqrt{3}\times\sqrt{3}R30°$ layer, flat Ag islands form in the Stranski-Krastanov (SK) growth mode.[2-5]

The question of the coverage and structure of the $\sqrt{3}\times\sqrt{3}R30°$ layer itself, however, is not at all settled, with different works giving various coverages, Θ, in the range $\frac{2}{3} \leq \Theta \leq 1$ monolayer (ML). In many of these determinations the question of the coverage has been treated as somewhat secondary, although each structural model proposed has had a definite coverage. There have been several "structure determinations" by scanning tunneling microscopy[6,7] (STM), low- and medium-energy ion scattering,[8,9] surface x-ray diffraction,[10,11] low-energy electron diffraction[10] (LEED), and photoelectron diffraction.[13,14] The corresponding structural models have largely been based on honeycomb structures of Ag ($\Theta = \frac{2}{3}$),[6,14] or trimer structures of Ag embedded in a honeycomb of Si ($\Theta = 1$).[7-11] According to one LEED experiment,[12] the Ag atoms are not ordered, and the x-ray results[10,11] are most sensitive to lateral Ag-Ag distances and indicate a range of azimuthal orientations.[11]

A honeycomb network has been observed using STM, but disagreement exists about whether the topmost layer consists of Ag with $\Theta = \frac{2}{3}$,[6] or Si with $\Theta = 1$.[7] The latter case was favored on the grounds that it could explain a semiconducting surface, but the nominal Ag coverage measured was $\Theta = 0.89 \pm 0.04$ ML for deposition at $T = 730$ K. A combined reflection high-energy electron diffraction and x-ray coverage determination[15] has been used to support tentatively models based on $\Theta = 1$, but the actual coverage measurements were given as 0.9 ± 0.1 ML at $T = 730$ K and 0.8 ± 0.1 ML at $T = 770$ K. The latest theoretical work does seem to favor $\Theta = 1$ ML quite strongly,[16] but we cannot be sure that all structural possibilities have been considered.

We present here coverage measurements of the $\sqrt{3}\times\sqrt{3}R30°$ structure as a function of substrate temperature during deposition (T_d) and subsequent annealing (T_a) using micro-Auger electron spectroscopy (AES). This technique allows us to measure the coverage of the $\sqrt{3}\times\sqrt{3}R30°$ layer at specific locations *between* the Ag islands of the SK growth. This work was prompted by broadbeam (~ 1 mm) measurements of AES break points as a function of T_d,[5] which showed that the coverage of the $\sqrt{3}\times\sqrt{3}R30°$ layer increased with T_d. We find that the coverage increases from $\sim \frac{2}{3}$ to 1 ML for $620 < T_d < 700$ K but changes much less on subsequent annealing at similar temperatures. We explain these results using a simple kinetic model in which, at coverages greater than $\frac{2}{3}$ ML, Ag adatoms must overcome a relatively well-defined activation energy E_r in order to join the $\sqrt{3}\times\sqrt{3}R30°$ layer. This kinetic process is in competition with adatom desorption at high T and with nucleation of islands at low T.

The acquisition of Auger electron spectra in the $EN(E)$ mode was done using a cylindrical mirror analyser (CMA) in an ultrahigh vacuum scanning electron microscope, which has been described previously.[3,17] In the present experiments 5 ML of Ag was deposited at 1 ML min^{-1}, as measured by a quartz crystal microbalance, onto a cleaned Si(111)7×7 substrate held at constant temperature in the range $610 \leq T_d \leq 800$ K, measured to ± 5 K using an infrared pyrometer. Spectra were collected from regions between the Ag islands, using a 30 keV, 0.1-μm-diam electron beam with current around 0.1 μA, at an angle of incidence of 73°.

Each spectrum was averaged for about 7 min, which allowed the area under the Ag peak (350 eV) to be measured to $\leq 4\%$ accuracy. Because the sample temperature was maintained by direct-current heating, the sample potential could change by a few volts on changing the temperature. This in turn led to a shift in measured peak positions in the $EN(E)$ spectrum. To correct for this, the first step in the processing of each spectrum was to align the energy scale to a single reference spectrum by comparing the positions of the main Ag peaks. In order to correct for any changes in transmission function due to misalignment of the retractable analyser between different spectra, each spectrum was fitted to the reference spectrum at three background regions.

These precautions reduced systematic variations in peak-to-background (P/B) ratios between different spectra in the same experiment to the same order as the random errors. Greater variability ($\sim \pm 10\%$) was observed between different experiments, where the sample and CMA had been repositioned. The background area B was found by extrapolating a linear least-squares fit to the background spectrum extending 450 eV above the peak. The P/B ratio is the ratio of the area in P above the background fit to the area below the fit. Each of the regions used in the data processing remained unchanged for all of the spectra. Calibration to a monolayer scale was done with reference to similar spectra reported previously for room-temperature deposits of Ag/Si(100) and (111).[3] This gave $P/B = 0.093 \pm 0.010$ for $\Theta = 1$ ML. The corresponding coverage scale is added to the right-hand side of Figs. 1 and 2. However, we should note that the main deductions we make only need the variation of the P/B ratio itself, which is internal to the present experiments.

Figure 1 shows the measured P/B ratio as a function of deposition temperature. After deposition the samples were cooled towards room temperature and the measurements taken with the sample at around 50 °C. There is a clear increase in measured coverage with deposition temperature in the range $620\ \text{K} \leq T_d \leq 700\ \text{K}$. No further change in coverage with temperature was observed outside this range. For $T_d > 700$ K, the mean coverage value is $\Theta = 1.05 \pm 0.08$ ML and for $T_d < 620$ K, $\Theta = 0.70 \pm 0.06$ ML.

A number of experiments were carried out to try to observe any change in coverage on annealing the sample after deposition. Care was taken to avoid sample contamination by minimizing exposure to the electron beam, in case any such contamination might hinder the diffusion of adatoms. Samples were annealed for up to several hours

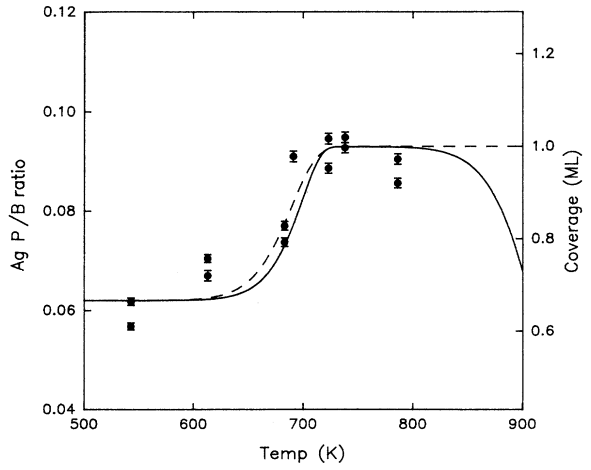

FIG. 1. Ag P/B ratio from the intermediate layer as a function of deposition temperature with deposition rate $R = 1.0$ ML min^{-1} and dose = 5.0 ML. Experimental points are shown as circles. The curves show the coverage in ML calculated with $E_r = 1.90$ eV and $E_e = 0.60$ eV, as discussed in the text. The solid curve is the result of a detailed calculation, while the dashed curve was calculated in the constant adatom approximation.

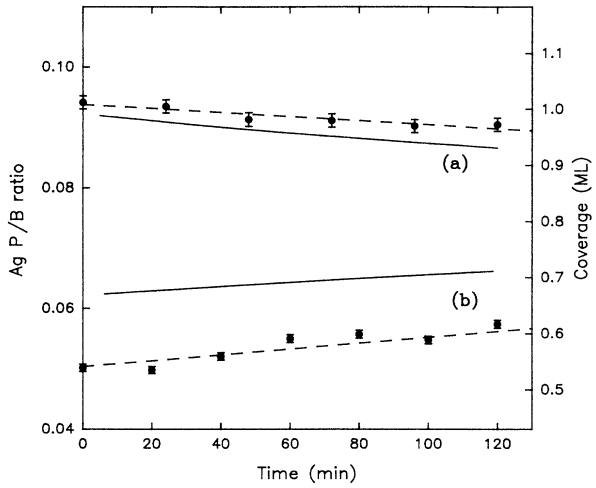

FIG. 2. Effect of annealing of the intermediate layer on Ag P/B ratio. The offsets of the calculated solid curves from the experimental data are a result of the error in fitting each experiment to an absolute coverage scale. The dashed curves represent linear least-squares fits to the data. (a) $T = 710$ K for both the deposition and the subsequent anneal. (b) Anneal temperature ≈ 700 K after deposition at 590 K.

at temperatures between 300 and 750 K, and the AES spectra were taken at temperature. Examples of two such experiments are shown in Fig. 2. In 2(a), the sample was deposited and annealed at 710 K, while in 2(b) deposition at 590 K was followed by annealing at 700 K. The origin of the time axis corresponds to the end of deposition. The dashed lines show a linear least-squares fit to the data. There is evidence of a decrease in the high initial coverage and an increase in the low initial coverage with time. Such changes are far smaller than the changes observed with deposition temperature and take place over several hours, in contrast to the 5-min deposition time.

The strong difference between deposition and annealing results shows clearly the necessity of a high adatom concentration to provide the thermodynamic driving force for completion of the $\sqrt{3}\times\sqrt{3}R30°$ layer. We propose a simple kinetic model to explain our results, whereby 2 Ag atoms per unit cell *on average* are incorporated into the $\sqrt{3}\times\sqrt{3}R30°$ layer when it is initially formed; but, while it is energetically favorable, by an amount E_e, for a third Ag atom also to join the layer, these atoms must overcome an activation energy E_r in order to do so. The energy levels for the incorporation of the third atom are shown in Fig. 3, together with the adatom adsorption energy E_a. In other words, we assume that during Ag deposition onto the clean Si surface, the first $\frac{2}{3}$ ML forms the $\sqrt{3}\times\sqrt{3}R30°$ layer and is relatively immobile, as has been shown by diffusion studies.[18] Silver atoms are then adsorbed on top of the layer. These adatoms are highly mobile and are quickly lost through desorption, capture by three-dimensional (3D) islands or incorporation into the intermediate layer. The role of such atomistic processes in island nucleation and growth has previously been extensively studied,[19] and we shall examine how our new model of the interaction between the layer and adatoms can be

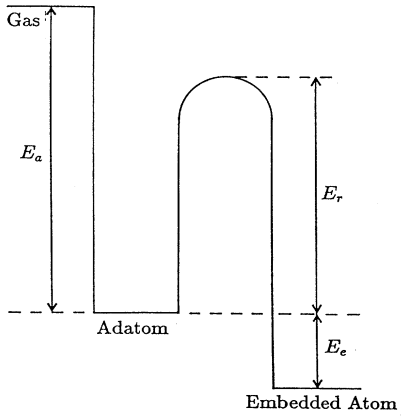

FIG. 3. Energy levels for incorporation of an Ag adatom into the intermediate layer ($n_e > \frac{2}{3}$) and desorption from the surface.

integrated into such calculations. First, however, we show our model can explain the experimental results with only minimal reliance on outside assumptions. Note that we do not assume homogeneity at the level of the unit cell, but only that adatoms move over long distances compared with the 0.1 μm diameter of the Auger beam. This is known to be the case from nucleation and diffusion studies.[3,18–20]

If the single adatom concentration above the intermediate layer is n_1 and the concentration of Ag atoms in the layer is n_e (both expressed in ML), then we can write the rate equation for incorporation into the intermediate layer (i.e., for $n_e > \frac{2}{3}$) as

$$\frac{dn_e}{dt} = n_1(1-n_e)\nu\exp(-E_r/kT) - n_e\nu \times\exp[-(E_r+E_e)/kT] , \quad (1)$$

where ν is the surface Ag atom vibrational frequency, which we take to be equal to 4.0×10^{12} Hz. Because of the high mobility of adatoms and constant nucleation density, we can make the approximation for the moment that n_1 is constant during deposition and falls by several orders of magnitude after deposition. If we also assume that E_e is large enough to make the second (reverse reaction) term in Eq. (1) negligible, we can integrate the first term analytically over the deposition period to find n_e as a function of deposition temperature T_d. From previous detailed calculations of the adatom concentration we take $n_1 = 0.08$ ML during deposition.[19] The results are shown in the dashed curve of Fig. 1 for $E_r = 1.9$ eV. We should note that the value of E_r obtained by fitting to the data is only weakly dependent on the value chosen for n_1; a change of an order of magnitude in the preexponential factor produces a change of 0.13 eV in the deduced value of E_r; the error is thus of the order ± 0.05 eV.

We now consider the annealing of a high-temperature deposit, shown in Fig. 2(a). Since n_e is close to 1, the first term in Eq. (1) can be ignored and the fall in coverage is due to atoms leaving the intermediate layer by overcoming the energy barrier (E_r+E_e). The gradient of the least-squares fit to the data is $-(7.3\pm2.4)\times10^{-6}$ ML s^{-1} which gives $(E_r+E_e) = 2.53\pm0.03$ eV and hence $E_e = 0.63\pm0.06$ eV.

The very small rate of change of coverage on annealing a low-temperature deposit [Fig. 2(b)] is direct evidence of the immediate large fall in n_1 when deposition is stopped. We can use Eq. (1) together with the measured values of E_r and E_e to find n_{1e}, the equilibrium value of n_1 after deposition is stopped, from the slope of Fig. 2(b). The measured gradient is $(1.0\pm0.4)\times10^{-5}$ MLs^{-1}, which implies $n_{1e} = (3.6\pm0.7)\times10^{-4}$ ML at $T = 700$ K. The adatom concentration in equilibrium with large Ag islands is given by

$$n_{1e} = K\exp-(L-E_a)/kT , \quad (2)$$

where K depends on the entropy difference between an adatom and an atom in a 3D island and $L = 2.95$ eV is the sublimation energy of bulk Ag. We can therefore find E_a from the measured value of n_{1e}. Taking $K = 3$ (appropriate for configurational entropy in a lattice gas with 3 equivalent sites) and using the measured value of n_{1e} at 700 K, we find $E_a = 2.41\pm0.05$ eV. Note how closely the three parameters, E_r, E_e, and E_a are constrained by the simple equations (1) and (2) and the data shown in Figs. 1 and 2. The value of E_a has been determined directly for the first time in the present work, although it has previously been inferred indirectly from nucleation and diffusion measurements.[19,20] The desorption energy for atoms in the $\sqrt{3}\times\sqrt{3}R30°$ layer is (E_a+E_e). This energy has been measured from isothermal-desorption experiments.[4,15] By comparing desorption rates in our model with the experimentally determined rates in Ref. 4, we find a desorption energy of 3.05 eV. This is in good agreement with the values of E_a and E_e already deduced.

We may now consider how this model for incorporation of atoms into the $\sqrt{3}\times\sqrt{3R}30°$ layer can be related to previous detailed calculations of nucleation and diffusion processes on the layer.[19,20] Capture by the intermediate layer takes place in competition with all the other loss processes for adatoms. The rate equation for these processes can be written as

$$\frac{dn_1}{dt} = R - n_1(\tau_a^{-1}+\tau_c^{-1}+\tau_e^{-1}) , \quad (3)$$

where R is the deposition rate in ML s^{-1}. The second and third terms in Eq. (3) represent adatom losses by desorption and capture by 3D islands, respectively. The final term corresponds to the loss of adatoms due to embedding in the $\sqrt{3}\times\sqrt{3}R30°$ layer, i.e., it is a shorthand way of representing Eq. (1).

The adsorption lifetime τ_a depends on the adsorption energy E_a, while the rate of adatom capture by islands (n_1/τ_c) depends on the island density and diffusion coefficient; so τ_c depends on the bond energy E_b of atoms in small clusters and the surface diffusion energy E_d. These energies have been determined previously by fitting Eq. (3), without the final term, to nucleation density and surface diffusion data.[19,20] For detailed computations here we have used $E_a = 2.45$ eV, $E_b = 0.05$ eV, and $E_d = 0.40$ eV, which are consistent with the previous analysis.

The solid curves in Figs. 1 and 2 were calculated using $E_r = 1.90$ eV and $E_e = 0.60$ eV. It is clear that these values, determined in the simple approximation described earlier, still give a good fit to the data in the more detailed calculation. At high deposition temperatures in Fig. 1,

the coverage begins to decrease as desorption becomes significant. Because E_r is only a little smaller than E_a, there is a relatively small temperature range in which the coverage is close to 1 ML. This is consistent with the fact that reported coverage measurements are frequently in the range 0.8–0.9 ML. The growth conditions to achieve $\Theta \approx 1$ ML are quite stringent, in that, not only must the temperature be in the necessary range, but there must also be a source of adatoms above the surface to fill the extra sites. We note that $\Theta = \frac{2}{3}$ ML was found from measurements of the spreading of finite patches at $T = 720$ K.[20] Under these conditions, where growth is by surface diffusion rather than by direct deposition, the adatom concentration is too low for the extra sites to be filled.

We have shown that the coverage of the $\sqrt{3}\times\sqrt{3}R30°$ layer, measured directly between Ag islands, can have values between $\sim \frac{2}{3}$ and 1 ML depending on the growth conditions. These results resolve many of the apparent contradictions in previous coverage measurements. Our results are well explained by a kinetic model which allows us to determine three characteristic energies for Ag adatoms: E_r, E_e, and E_a. They do not enable us to choose a specific structural or microstructural model of the intermediate layer. If the layer is homogeneous at the scale of the unit cell, they are consistent with some variant of the "embedded trimer" model where one of the three Ag atoms has a site symmetry distinct from the others and must overcome the activation energy E_r in order to produce measured coverages greater than $\frac{2}{3}$ ML. It is not necessarily surprising that initial diffraction studies showed no evidence of structural changes in the $\sqrt{3}\times\sqrt{3}R30°$ layer with coverage, since LEED I-V curves from a clean metastable Si $\sqrt{3}\times\sqrt{3}R30°$ surface have been shown to be very similar to those from the Ag/Si $\sqrt{3}\times\sqrt{3}R30°$ layer.[12]

If the layer is inhomogeneous at a microstructural level, then (a) the length scale involved is $\ll 0.1$ μm in our experiments and (b) the activation energy for incorporation, E_r which we measure, corresponds to the energy necessary to move the boundary between high- and low-coverage regions on the surface. In this case the various microstructural possibilities could only be unravelled by microscopic observations at even higher spatial resolution, or by diffraction profile analysis.

Recently,[21] this latter technique has been used to show that domain coarsening does indeed take place in submonolayer deposits on the 5 minute timescale, and that there is a rapid transition in the coarsening rate, in exactly the same temperature range $623 < T < 723$ K as the coverage changes seen here. Electron microscope images[22] show triangular regions with a range of contrast at submonolayer coverages, and there is evidence of the effects of steps in the growth of the $\sqrt{3}\times\sqrt{3}R30°$.[23] However, a simple juxtaposition of a $\Theta = 1$ phase and a $\Theta = 0$ phase is not thermodynamically possible (at $T > 0$ K), which implies that microstructural variability must be accompanied by coverage variations at the unit-cell level. The model we present has been used to deduce energies which are insensitive to these fine-scale structural uncertainties, but the interpretation of E_r is dependent on the structural and microstructural model preferred.

We thank the SERC for supporting this work and Dr. C. J. Harland for technical assistance.

*Also at Arizona State University, Tempe, AZ 85287.

[1]G. Lelay, Surf. Sci. **132**, 169 (1983); M. Hanbücken and G. Lelay, Surf. Sci. **168**, 122 (1986), and this volume generally.

[2]Y. Gotoh, S. Ino, and H. Komatsu, J. Cryst. Growth **56**, 498 (1982).

[3]M. Hanbücken, M. Futamoto, and J. A. Venables, Surf. Sci. **147**, 433 (1984).

[4]G. Lelay, M. Manneville, and R. Kern, Surf. Sci. **72**, 405 (1978).

[5]G. Lelay, A. Chauvet, M. Manneville, and R. Kern, Appl. Surf. Sci. **9**, 190 (1981); Y. Gotoh, A. Chauvet, M. Manneville, and R. Kern, Jpn. J. Appl. Phys. **20**, L853 (1981).

[6]R. J. Wilson and S. Chiang, Phys. Rev. Lett. **58**, 369 (1987); **58**, 2575 (1987); J. Vac. Sci. Technol. A **6**, 398 (1988), **6**, 800 (1988).

[7]E. J. van Loenen, J. E. Demuth, R. M. Tromp, and R. J. Hamers, Phys. Rev. Lett. **58**, 373 (1987); J. E. Demuth, E. J. van Loenen, R. M. Tromp, and R. J. Hamers, J. Vac. Sci. Technol. B **6**, 18 (1988).

[8]T. L. Porter, C. S. Chang and I. S. T. Tsong, Phys. Rev. Lett. **60**, 1739 (1988).

[9]M. Copel and R. M. Tromp, Phys. Rev. B **39**, 12688 (1989).

[10]T. Takahashi, S. Nakatani, N. Okamoto, T. Ishikawa, and S. Kikuta, Jpn. J. Appl. Phys. **27**, L753 (1988).

[11]E. Vlieg, A. W. Denier van der Gon, J. F. van der Veen, J. E. McDonald, and C. Norris, Surf. Sci. **209**, 100 (1989).

[12]W. C. Fan, A. Ignatiev, H. Huang, and S. Y. Tong, Phys. Rev. Lett. **62**, 1516 (1989).

[13]S. Kono, T. Abukawa, N. Nakamura, and K. Anno, Jpn. J. Appl. Phys. **28**, L1278 (1989).

[14]E. L. Bullock, G. S. Herman, M. Yamada, D. J. Friedman, and C. S. Fadley, Phys. Rev. B **41**, 1703 (1990).

[15]S. Hasegawa, H. Daimon, and S. Ino, Surf. Sci. **186**, 138 (1987).

[16]Y. G. Ding, C. T. Chan, and K. M. Ho, Phys. Rev. Lett. **67**, 1454 (1991).

[17]C. J. Harland and J. A. Venables, Ultramicroscopy **17**, 9 (1985).

[18]M. Hanbücken, T. Doust, O. Osasona, G. Lelay, and J. A. Venables, Surf. Sci. **168**, 133 (1986).

[19]J. A. Venables, Phys. Rev. B **36**, 4153 (1977); J. A. Venables, G. D. T. Spiller, and M. Hanbücken, Rep. Prog. Phys. **47**, 399 (1984).

[20]J. A. Venables, T. Doust, and R. Kariotis, Mater. Res. Symp. **94**, 3 (1987); T. Doust, Ph.D. thesis, University of Sussex, 1988; T. Doust, F. L. Metcalfe, and J. A. Venables, Ultramicroscopy **31**, 116 (1989).

[21]J. K. Zuo and J. F. Wendelken, Phys. Rev. Lett. **66**, 2227 (1991).

[22]A. Endo, H. Daimon, and S. Ino, in *Proceedings of the 12th International Congress on Electron Microscopy,* edited by L. D. Peachey and D. B. Williams (San Francisco Press, San Francisco, 1990), Vol. 1, p. 304.

[23]K. Takayanagi, (unpublished); S. Y. Tong and H. Huang, Surf. Sci. **243**, L46 (1991).